Rapid Slice-by-Slice Calculation of Susceptibility-Induced B_0 Map in the Fourier Domain

Seung-Kyun Lee[1], and Ileana Hancu[1]
[1]*GE Global Research, Niskayuna, NY, United States*

Introduction: Susceptibility-induced off-resonance field in high field MRI can be accurately calculated in the spatial domain by adding dipolar fields from all the magnetized voxels in the subject in the main magnetic field. For 3D calculation, a much faster, Fourier-domain method [1,2] has been used to calculate subject-induced B_0 inhomogeneity in brain [3] and a single breast [4]. Extension of the method to high resolution body imaging requires a large computer memory (> gigabyte) to handle large matrices. In this work we introduce a 2D Fourier-based, slice-by-slice calculation of susceptibility-induced B_0 field which is highly memory-efficient and attains comparable speed of calculation in a small number of slices. The method naturally allows comparison of contributions from different body parts to the B_0 map of a given slice.

Theory: The z-component of the dipolar magnetic field at (x, y, z) contributed by a single susceptibility voxel of volume Δv at (x', y', z') is

$$B_d(x,y,z,;x',y',z') = B_0\,\Delta v\,\chi(x',y',z')\cdot\left\{\frac{1}{4\pi}\cdot\frac{2(z-z')^2-(x-x')^2-(y-y')^2}{[(x-x')^2+(y-y')^2+(z-z')^2]^{5/2}}\right\} \quad (1)$$

where B_0 is the main magnetic field and χ is the susceptibility. Consider two axial slices at z and z'. In this case, double integral of Eq. (1) over x' and y' gives the dipolar field map on the slice at z contributed by the susceptibility of the slice at z'. This integral can be performed in the Fourier domain, in which convolution implied in Eq. (1) is conveniently replaced by multiplication of susceptibility and dipolar field functions:

$$\tilde{B}_d(k_x,k_y,z;z') = B_0\Delta z'\tilde{K}(k_x,k_y,h)\tilde{\chi}(k_x,k_y,z'), \qquad h\equiv z-z'. \quad (2)$$

Here ~ indicates Fourier transform with respect to the variables denoted with letter k, $\tilde{K}$ is the Fourier transform of the quantity in { } in Eq. (1) with respect to $x-x'$ and $y-y'$, and $\Delta z'$ is the thickness of the susceptibility slice. The function $\tilde{K}$ turns out to have a simple form,

$$\tilde{K}(k_x,k_y,h) = -\frac{2}{3}\delta(h)+\frac{1}{2}k\exp(-k|h|), \quad k\equiv\sqrt{k_x^2+k_y^2} \quad (3)$$

The singularity at $h=0$ in the Dirac delta function $\delta(h)$ is avoided in practice by defining $\tilde{K}(k_x,k_y,0)\equiv -2/(3\Delta)+(1/\Delta)\{1-\exp(-k\Delta/2)\}$ which is the average of Eq. (3) over $-\Delta/2 < h < \Delta/2$ where Δ is the thickness of the susceptibility slice at $h = 0$.

For a sagittal pair of slices, Eqs (2,3) are replaced by the following,

$$\tilde{B}_d(x,k_y,k_z;x') = B_0\Delta x'\tilde{K}(h,k_y,k_z)\tilde{\chi}(x',k_y,k_z), \qquad h\equiv x-x' \quad (4)$$

$$\tilde{K}(h,k_y,k_z) = \frac{1}{3}\delta(h)-\frac{k_z^2}{2k}\exp(-k|h|), \quad k\equiv\sqrt{k_y^2+k_z^2} \quad (5)$$

with the provision $\tilde{K}(0,k_y,k_z)\equiv 1/(3\Delta)-k_z^2/(k^2\Delta)\{1-\exp(-k\Delta/2)\}$. Figure 1 shows the result of applying Eqs. (2-5) to calculation of the dipolar field map of a uniform sphere. Figure 2 shows application of the method to the breast B_0 map in a susceptibility-segmented female human body model; axial dipolar field contributions from 578 slices are easily compared.

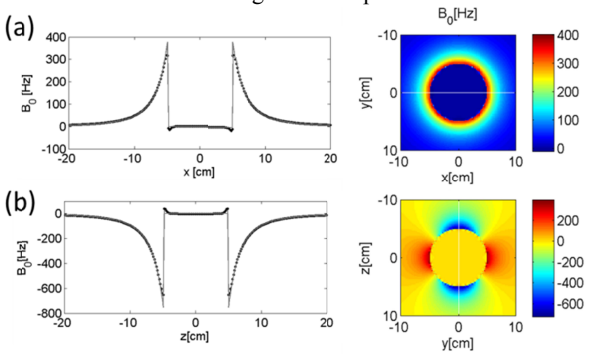

Figure 1. Calculated off-resonance field in and around a homogeneous sphere with χ = –9 ppm at 3 T. Dotted and solid lines in the plot on the left represent field profiles obtained by the proposed method and by analytical calculation, respectively. (a) Axial mid-plane. (b) Sagittal mid-plane.

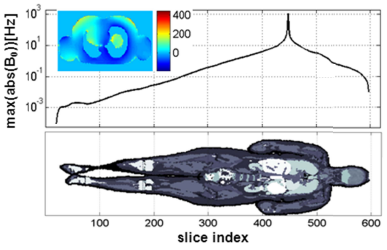

Figure 2. Susceptibility-induced B_0 map at 3 T in an axial slice through breast (inset) contributed from all slices in Visible Woman. Susceptibility segmentation was: air/lung/tissue = 0/–2.25/ –9 ppm.

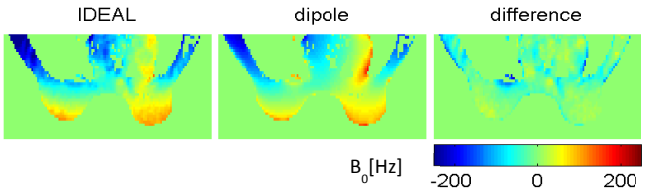

Figure 3. Comparison of breast B_0 maps produced by IDEAL (left), and by the proposed method (middle). For IDEAL, the scanner's shim field was calibrated out off-line. Anatomy-based dipolar B_0 map was obtained from susceptibility-segmented 3D image covering 50cm S/I from belly to neck. In-plane matrix was 512×512 including buffer; slice thickness was 6 mm.

In vivo validation: A healthy volunteer was scanned for a breath-held 3D anatomical image in the upper torso and Dixon's fat-water separation-based B_0 mapping (IDEAL[5]) in the breast. Our method was applied to the air/lung/tissue-segmented anatomical image to produce susceptibility-induced B_0 map in a single breast slice. The calculated and measured B_0 maps are compared in Fig. 3. Good agreement is observed. The difference can be due to motion in the non-breath-held IDEAL scan, segmentation error, background field, and any dipolar B_0 contributed by tissue outside the 50 cm imaged anatomy. All calculations were done with Matlab (Mathworks, MA) running on a 32 bit laptop PC with 2 GB of RAM.

Discussion: In the 3D Fourier method, susceptibility matrix representing upper torso at 1.5 mm isotropic resolution can be as large as 512×512×1024, including buffer volumes to avoid Fourier replica effect. With double precision data type, such matrix occupies 2 GB contiguous memory. In contrast, the 2D method would do with only a few, 2 MB matrices in this example. In terms of speed, 3D FFT on a $N_x\times N_y\times N_z$ matrix takes calculation time of $N_xN_yN_z\log(N_xN_yN_z)$. If B_0 map of a single slice is desired, the 2D method takes $N_xN_yN_z\log(N_xN_y)$, a clear gain over 3D. The advantage also lies in the fact that in 2D calculation, one can use thicker slices to represent susceptibility in distant slices, which can substantially reduce the number of summations in the slice direction. Due to the long range nature of the dipolar magnetic field, susceptibility in relatively distant voxels can often generate measureable B_0 effects. Examples are lung-volume-induced B_0 offset in neuroimaging and metallic implants. Our method can be useful in these cases to allow rapid patient-specific shim calculations with greater computational efficiency and flexibility.

Acknowledgement: This work was supported by the NIH grant 1R01CA154433-01A1. **References:** [1] Salomir R et al. Concepts Magn Reson 19B:26-34 (2003) [2] Marques JP, Bowtell R. Conepts Magn Reson 25B:65-78 (2005) [3] Koch KM et al. Phys Med Biol 51:6381-6402 (2006) [4] Jordan CD et al. Proc. ISMRM 17:2125 (2009) [5] Reeder SB et al. MRM 51:35-45 (2004)